

Yanbu Wang¹

Yan Geng^{2,*}

Wei Wang²

Chao Wang³

Qi Zhang²

REHABILITATION OF ROWING ATHLETES DURING THE FORMATION OF RESPIRATORY RHYTHMS IN COURSE OF BONE TISSUE PROSTHETICS

REHABILITACIJA VESLAČEV MED NASTAJANJEM DIHALNIH RITMOV PRI PROTETIKI KOSTNEGA TKIVA

ABSTRACT

Athletes who are engaged in rowing are subject to a number of occupational health problems that require not only long-term rehabilitation but also long-term recovery. The purpose of the article is to highlight the rehabilitation of rowing athletes during the formation of respiratory rhythms in course of bone tissue prosthetics. The aspect of the restoration of disturbed breathing rhythms and the activity of the cardiovascular system is of particular relevance. Since disorders of the cardiovascular system usually take place when associated physical damage occurs, the issue of forming a model of medical intervention during operations and rehabilitation activities is of primary importance. The main research method was the experimental method. With its help, experimental measurements and analysis of the obtained results were carried out. The novelty of the study is determined by the fact that the formation of a system of rehabilitation measures should be determined by the requirements for the achievement of previously shown results. The authors determine the structure of the model, its practical application and the formation of a graphic model on its basis that will be used when replacing parts of the skeletal support. It was determined that this allows to form not only stable functioning support, but also the respiratory systems, and thus lay the foundation for the athlete's further physical rehabilitation for practical activities and return to sports. The practical significance of the subject matter is determined by the need to form adaptive potential, which will allow athletes to maintain positive dynamics of performances in the future at the level of international competitions.

Keywords: restoration, cardiovascular system, fracture, osteosynthesis, treatment

¹*Department of the Physical Training, Beijing Sport University, Beijing, China*

²*Department of the Olympic Sport History and Theory, National University of Ukraine on Physical Education and Sport, Kyiv, Ukraine*

³*Department of the High Performance Sport, Beijing Sport University, Beijing, China*

IZVLEČEK

Športniki, ki se ukvarjajo z veslanjem, so podvrženi številnim poklicnim zdravstvenim težavam, ki poleg dolgotrajne rehabilitacije zahtevajo tudi dolgotrajno okrevanje. Namen članka je osvetliti rehabilitacijo veslačev med oblikovanjem dihalnih ritmov pri protetiki kostnega tkiva. Vidik ponovne vzpostavitve motenega ritma dihanja in delovanja srčno-žilnega sistema je še posebej pomemben. Ker do motenj srčno-žilnega sistema običajno pride ob pojavu pridruženih telesnih poškodb, je vprašanje oblikovanja modela medicinskega posega med operacijami in rehabilitacijskimi aktivnostmi bistvenega pomena. Glavna raziskovalna metoda je bila eksperimentalna metoda. Z njegovo pomočjo so bile izvedene eksperimentalne meritve in analiza dobljenih rezultatov. Novost študije določa dejstvo, da je treba oblikovanje sistema rehabilitacijskih ukrepov določiti z zahtevami za doseganje predhodno prikazanih rezultatov. Avtorji določijo zgradbo modela, njegovo praktično uporabo in na njegovi osnovi oblikovanje grafičnega modela, ki bo uporabljen pri zamenjavi delov skeletnega nosilca. Ugotovljeno je bilo, da to omogoča oblikovanje ne le stabilne podpore za delovanje, temveč tudi dihalnih sistemov in s tem postavlja temelje za nadaljnjo fizično rehabilitacijo športnika za praktične aktivnosti in vrnitev v šport. Praktični pomen predmeta je določen s potrebo po oblikovanju adaptivnega potenciala, ki bo športnikom omogočil ohranjanje pozitivne dinamike uspešnosti v prihodnosti na ravni mednarodnih tekmovanj.

Ključne besede: obnova, kardiovaskularni sistem, zlom, osteosinteza, zdravljenje

Corresponding author:* Yan Geng,
Department of the Olympic Sport History and Theory,
National University of Ukraine on Physical Education and
Sport, Kyiv, Ukraine

E-mail: yageng350@gmail.com

<https://doi.org/10.52165/kinsi.29.1.177-202>

INTRODUCTION

Plate osteosynthesis holds a significant place in the surgical treatment of injuries and diseases of the musculoskeletal system to achieve high-quality results in rehabilitation after diseases and surgical interventions on the cardiovascular system (Gart and Wiedrich, 2017). An ideal fixator is one that, with minimal additional trauma to the soft and bone tissues, preserves the immobility of the fragments, and provides the function and supportability of the damaged limb throughout the entire treatment period (Malempati et al., 2015). Fixators should be produced from biologically inert materials (Bjerke et al., 2014).

Fixator designs must be biomechanically justified (Hilliard et al., 2017). In the presence of alternating stresses, the destruction of material occurs at stresses significantly lower than the ultimate stress limit under a single static loading (Riley and Callahan, 2019). There are situations when the fixator does not withstand a long dynamic load (Bakrac, 2003). Stable plate osteosynthesis is an effective treatment for fractures (Hawson, 2011). A feature of the method is the creation of a large safety margin, which allows for early movements, thereby combining periods of consolidation and restoration of limb function (Hart et al., 1998). The scale of modern injuries has transformed this problem from medical to social (Arvinen-Barrow et al., 2014). Injuries in developed countries are the third leading cause of death and disability (Rudenko et al., 2015). Damage to the musculoskeletal system is detrimental to human health, which leads to significant material costs (Carlson, 2009). Annually, about 10% of the population receives bone fractures, and 0.5-16% of these patients experience non-union (Hagerman et al., 1995). An analysis of modern domestic and foreign literature indicates that there is no universal treatment method (Hagerman et al., 1995). Bone osteosynthesis is performed using structures such as wire, and metal rings (Arvinen-Barrow et al., 2015). This method has insufficiently strong fixation and does not find an independent application, but can be used together with other methods (Karpel et al., 2021).

The design of the plates provides for the introduction of screws in one area (Grindem et al., 2018). Multi-fragmentary fractures are less sensitive to displacements; the absolute displacement separates into many insignificant relative displacements between individual fragments (Bejar et al., 2019). The situation with simple fractures is more critical (Wilk et al., 2016). For simple diaphyseal fractures, bone osteosynthesis should be used, with anatomical repositioning and interfragmentary compression (Lu and Hsu, 2013). Today, there are many osteosynthesis systems, but all of them have certain disadvantages (Abassi et al., 2019). Given

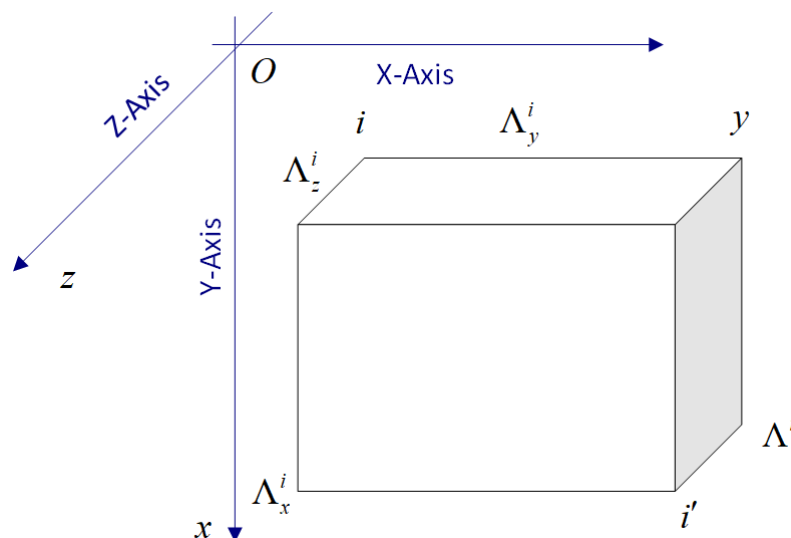
these circumstances, it is advisable to continue work on improving osteosynthesis systems (Wasik et al., 2015). The purpose of the article is to highlight the rehabilitation of rowing athletes during the formation of respiratory rhythms in course of bone tissue prosthetics.

METHODS

If the components of the displacement at the most dangerous point are known (the projections of the total vector on the coordinate axis (Fig. 1), then the condition will be written as:

$$\Lambda_{max} = \sqrt{(\Lambda_x^i)^2 + (\Lambda_y^i)^2 + (\Lambda_z^i)^2} |_{max} \leq [\Lambda] \quad (1)$$

Figure 1. Directions of coordinate axes and components of the main vector of cell displacements.



The components of the displacements in equation (1) are determined mainly by the influence of such forces: P_1 – force acting along the longitudinal axis of the bone (for the lower extremities – this is mainly the strength of a person’s weight); P_2 – lateral force (muscle strength, limb weight in the supine position of the injured); P_3 – force that affects the foot when walking (the action of muscles during rotational movements of the body during walking, the weight of the foot in the supine position of the victim) and causes torsion deformities of the limb bones.

Due to the action of these forces, bending moments and torsion moment appear:

$$M_k = P_k e_k \quad (2)$$

where e_k – the distance from the line of action of the corresponding force to the place of fixation of the fracture; $k=1,2,3$ – designations of forces and corresponding moments.

Use of forces P_1, P_2, P_3 and corresponding bending moments M_1, M_2, M_3 , acting in the fracture area. Presented: e_1 – distance from the line of action of force P_1 to the means of fixation; e_2 – distance from the line of action of force P_2 in the middle of the fracture; e_3 – distance from the line of action of force P_3 to the means of fixation. Thus, each component of the main linear displacement vector Λ^i depends on three concentrated forces and three moments of force. Let us denote: $\Lambda_k^i(\Lambda_1^i, \Lambda_2^i, \Lambda_3^i)$ – absolute displacement of point “i”, caused by forces P_k ; $\Lambda_j^i(\Lambda_x^i, \Lambda_y^i, \Lambda_z^i)$ – projections of the full displacement of a point “i” on axis “j”; Λ_{jk}^i – projection on the axis “j” of absolute displacements Λ_k^i .

It should be noted that most osteosynthesis systems are located on the lateral (external to the centre of the body) or on the medial (internal) side of the bone. The axis of the longitudinal force P_i passes through the frontal (the one that divides the body into the front and back) area of the bone. In the future will be considered the case when the line of action of the most dangerous force P_2 will also lie in the frontal plane. Therefore, displacements arising due to these forces and corresponding moments must be added algebraically.

It should also be noted that the direction of action of external forces is unknown in advance. Therefore, in the future will be considered the most dangerous arrangement of forces P_1, P_2, P_3 , when the directions of the projections of displacement from all these forces coincide. In this regard, when constructing the criteria of functional reliability, it should be assumed that all components of the displacement vector have the same sign. Let us denote by λ reduced displacements as the ratio of the absolute values of displacements to the acting forces, and by $\bar{\lambda}$ displacements as the ratio of absolute values of displacements to current moments:

$$\lambda_{jk}^i = \frac{\Lambda_{jk}^i}{P_k} \quad (3)$$

$$\bar{\lambda}_{jk}^i = \frac{\Lambda_{jk}^i}{M_k} \quad (4)$$

The given displacements are determined experimentally by measuring displacements under the action of the corresponding forces and moments, for example, by digital recording using a camera. It should be noted that to determine the displacement λ_{jk}^i absolute displacement must be measured in the absence (or at least minimising) of the bending moment. This is done by applying a load to the system near the fixing means. When determining the given displacements $\bar{\lambda}_{jk}^i$ from general absolute displacements, it is necessary to remove displacements arising under the action of only concentrated forces.

If the given displacements are known, then the components of the absolute displacements can be determined for any values of the components of the force vector P_k and corresponding components of the moment vector M_k . Projection of general displacement Λ^i the entire X is defined as follows:

$$\Lambda_x^i = \lambda_{x1}^i P_1 + \lambda_{x2}^i P_2 + \lambda_{x3}^i P_3 + \bar{\lambda}_{x1}^i M_1 + \bar{\lambda}_{x2}^i M_2 + \bar{\lambda}_{x3}^i M_3 \quad (5)$$

Projection of cell displacement Λ^i on axis Y and Z is defined similarly:

$$\Lambda_j^i = \sum_{k=1}^3 P_k (\lambda_{jk}^i + \bar{\lambda}_{jk}^i e_k) \quad (6)$$

The condition of functional reliability using the maximum linear mutual displacement as a criterion is written in compressed form:

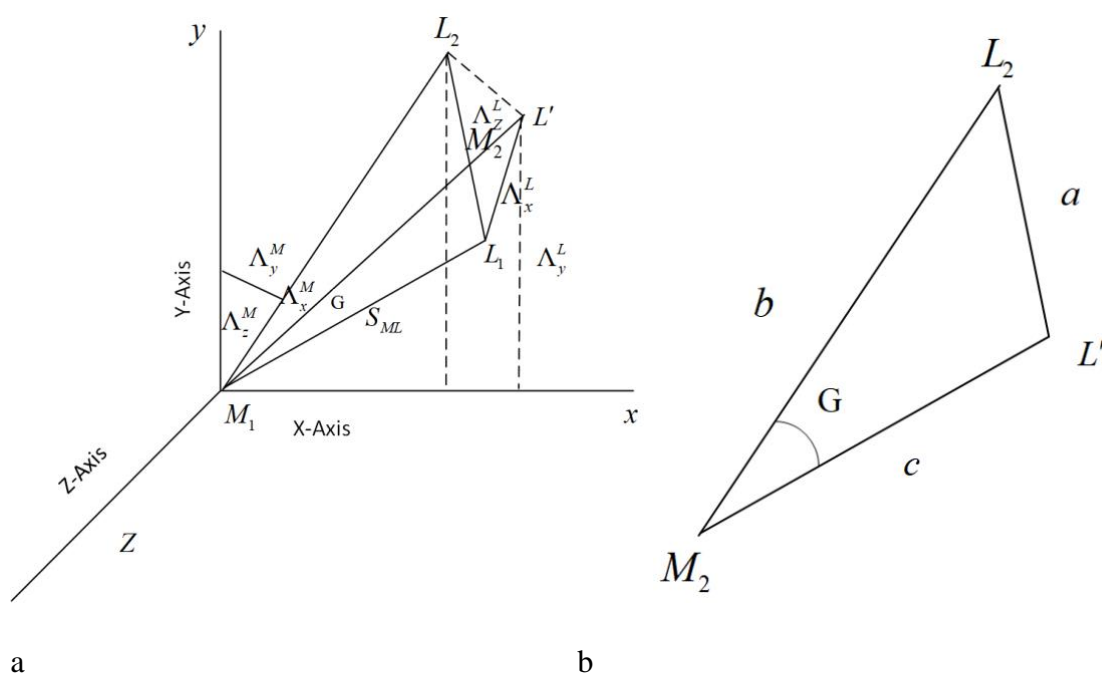
$$\Lambda_{max} = \left\{ \sum_{j=1}^3 \left[\sum_{k=1}^3 P_k (\lambda_{jk}^i + \bar{\lambda}_{jk}^i e_k) \right]^2 \right\}^{1/2} \quad |_{max} \leq [\Lambda] \quad (7)$$

Denote (Fig.2 a): G – angle of rotation of the line that connects two opposite fracture points M, L ; M_1, L_1 – the position of two opposite fracture points to the application of the load;

M_2, L_2 – position of two opposite fracture points after application of load; L' – position of point L after application of the load without taking into account the rotation of the fracture (parallel movement of the segment M_1, L_1); S_{ML} – distance between points M, L in different positions; $\Lambda_X^M, \Lambda_Y^M, \Lambda_Z^M$ – displacement projection of point M on the coordinate axes; $\Lambda_X^L, \Lambda_Y^L, \Lambda_Z^L$ – displacement projection of point L on the coordinate axes; $L'L_2$ – displacement of point L only due to the mutual rotation of the parts of the fracture.

$$S_{ML} = M_1L_1 = M_2L_2 = M_2L' \tag{8}$$

Figure 2. Detailed (a) and simplified (b) diagram of movements of fracture points and rotation angles of fracture parts.



From the triangle $L'L_2M_2$ (Fig. 2 b):

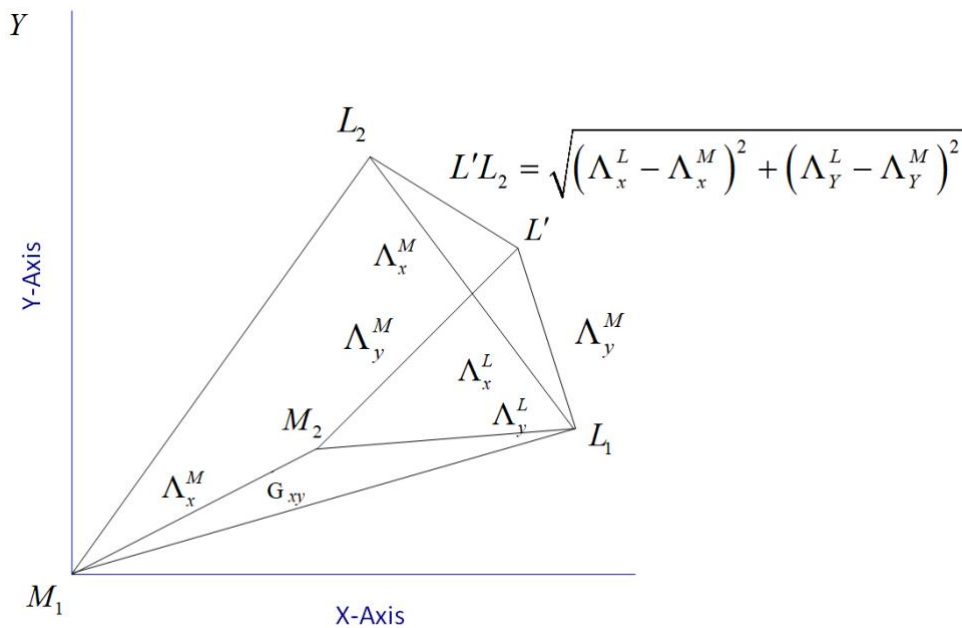
$$|L'L_2| = \sqrt{(\Lambda_x^L - \Lambda_x^M)^2 + (\Lambda_y^L - \Lambda_y^M)^2 + (\Lambda_z^L - \Lambda_z^M)^2} \tag{9}$$

where, given the designations shown in Fig. 2:

$$|L'M_2| = S_{ML}; |L_2M_2| = S_{ML} \tag{10}$$

Explanations for formula (10) are given in Fig. 3, where for illustrative purposes are shown the projections of vectors $M_1M_2, L_1L_2, L'L_2$ and projections of the corresponding displacements on the plane XOY .

Figure 3. Projections of displacement vectors of fracture points on a plane XOY .



In the final form, the angle of rotation of the parts of the fracture is defined as:

$$G = \arccos \left(1 - \frac{|L'L_2|^2}{2S_{ML}^2} \right) \tag{11}$$

Functional reliability condition (2), using the maximum mutual angle as a criterion of rotation of the fracture parts (11), looks like this:

$$G_{max} = \arccos \left\{ 1 - \frac{1}{2S_{ML}^2} \sum_{j=1}^3 \left[\sum_{k=1}^3 P_k \left((\lambda_{jk}^L - \lambda_{jk}^M) + (\bar{\lambda}_{jk}^L - \bar{\lambda}_{jk}^M) e_k \right) \right] \right\} |_{max} \leq [G] \tag{12}$$

RESULTS AND DISCUSSION

The process of rehabilitation of the injured is accompanied by exposure of limbs to cyclically acting loads (walking, exercise). In this case, the mutual displacements of the opposite parts of

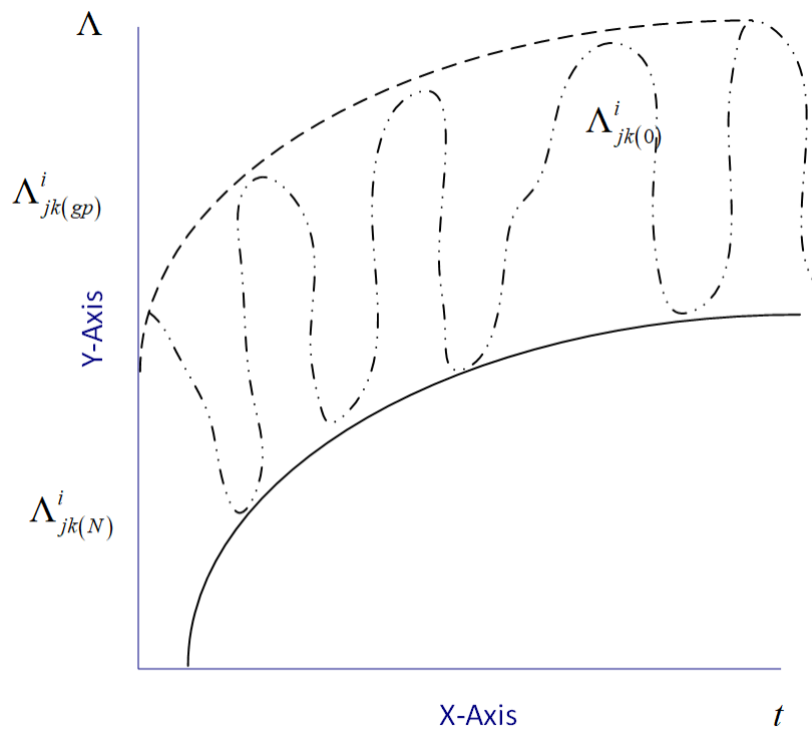
the fracture can significantly increase, and the condition of functional reliability should take into account the deformations (displacements) that accumulate in the osteosynthesis system when cyclic loads are applied:

$$\Lambda_{max}(N) = \left\{ \sum_{j=1}^3 \left[\sum_{k=1}^3 P_k \left((\lambda_{jk(0)}^i + \lambda_{jk(N)}^i) + (\bar{\lambda}_{jk(0)}^i + \bar{\lambda}_{jk(N)}^i) e_k \right) \right]^2 \right\}^{1/2} \quad |_{max} \leq [\Lambda] \quad (13)$$

In (13), it was taken into account that the components of the point displacement consist of instantaneous displacement of cells $\Lambda_{jk(0)}^i$ and displacement of cells $\Lambda_{jk(N)}^i$, arising during the term of N load cycles (Figs. 3, 4):

$$\Lambda_{jk}^i = \Lambda_{jk(0)}^i + \Lambda_{jk(N)}^i \quad (14)$$

Figure 4. Diagram of development of displacements of adjacent points and accepted notation.



This can be expressed through reduced displacements arising due to the action of forces (λ_{jk}^i) and moments $(\bar{\lambda}_{jk}^i)$

$$\lambda_{jk}^i = \lambda_{jk(0)}^i + \lambda_{jk(N)}^i \quad (15)$$

$$\bar{\lambda}_{jk}^i = \bar{\lambda}_{jk(0)}^i + \bar{\lambda}_{jk(N)}^i \quad (16)$$

where, as in (13, 14), the index “0” means the instantly elastic component, the index N – accumulated displacements:

$$\lambda_{jk(0)}^i = \frac{\Lambda_{jk(0)}^i}{P_k}; \lambda_{jk(N)}^i = \frac{\Lambda_{jk(N)}^i}{P_k} \quad (17)$$

$$\bar{\lambda}_{jk(0)}^i = \frac{\Lambda_{jk(0)}^i}{M_k}; \bar{\lambda}_{jk(N)}^i = \frac{\Lambda_{jk(N)}^i}{M_k} \quad (18)$$

The most interesting from a practical point of view are the displacements of the fracture points, which accumulate under the action of a significant number of load cycles. In this case, in formula (13), displacements are given; it is advisable to replace the displacements that occurred on the N -th cycle with the limiting ones (under the influence of the maximum number of cycles):

$$\Lambda_{max} = \left\{ \sum_{j=1}^3 \left[\sum_{k=1}^3 P_k \left(\left(\lambda_{jk(0)}^i + \lambda_{jk(gp)}^i \right) + \left(\bar{\lambda}_{jk(0)}^i + \bar{\lambda}_{jk(gp)}^i \right) e_k \right) \right]^2 \right\}^{1/2} \quad |_{max} \leq [\Lambda] \quad (19)$$

where indicated:

$$\lambda_{jk(gp)}^i = \frac{\Lambda_{jk(gp)}^i}{P_k}; \bar{\lambda}_{jk(gp)}^i = \frac{\Lambda_{jk(gp)}^i}{M_k} \quad (20)$$

Given that:

$$P_k \left(\lambda_{jk(0)}^i + \bar{\lambda}_{jk(0)}^i e_k \right) = \Lambda_{jk(0)}^i \quad (21)$$

$$P_k \left(\Lambda_{jk(gp)}^i + \bar{\Lambda}_{jk(gp)}^i e_k \right) = \Lambda_{jk(gp)}^i \quad (22)$$

equation (22) can be written in this way:

$$\Lambda_{max} = \sqrt{\sum_{j=1}^3 \left[\sum_{k=1}^3 P_k k_{jk}^i \left(\lambda_{jk}^i + \bar{\lambda}_{jk(0)}^i e_k \right) \right]} \Big|_{max} \leq [\Lambda] \tag{23}$$

where:

$$k_{jk}^i = 1 + \frac{\Lambda_{jk(gp)}^i}{\Lambda_{jk(0)}^i} \tag{24}$$

a ratio of cyclic creep, which shows an increase in the total displacement that occurs under cyclic loading, compared with the movement of the load at the single load.

Under the action of cyclic loads, the angles of mutual rotation of the parts of the fracture can increase significantly. These changes compared to angles arising under the action of one-time

loads can be taken into account by adding to instantly elastic displacements $(\Lambda_{jk(0)}^L, \Lambda_{jk(0)}^M)$ of viscoelastic origin (displacement $\Lambda_{jk[N]}^L$ and $\Lambda_{jk(N)}^M$, arising for N load cycles) of points L, M respectively. As in the case of linear displacements, this can be expressed in terms of displacements that arise due to the action of forces $(\lambda_{jk}^L, \lambda_{jk}^M)$ and moments $(\bar{\lambda}_{jk}^L, \bar{\lambda}_{jk}^M)$:

$$G_{max}(N) = \text{arc cos} \left\{ 1 - \frac{1}{2S_{ML}^2} \sum_{j=1}^3 \left[\sum_{k=1}^3 P_k \left((\lambda_{jk(0)}^L + \lambda_{jk(N)}^L - \lambda_{jk(0)}^M - \lambda_{jk(N)}^M) + (\bar{\lambda}_{jk(0)}^L + \bar{\lambda}_{jk(N)}^L - \bar{\lambda}_{jk(0)}^M - \bar{\lambda}_{jk(N)}^M) e_k \right) \right]^2 \right\} \Big|_{max} \leq [G] \tag{25}$$

In the equation (25), the expressions for the displacement components (9) – (11) are applied with the replacement of the notation of the point “ i ” by the points $= L? , = M? :$

$$\Lambda_{jk}^L = \Lambda_{jk(0)}^L + \Lambda_{jk(N)}^L; \Lambda_{ik}^M = \Lambda_{jk(0)}^M + \Lambda_{jk(N)}^M; \tag{26}$$

$$\lambda_{jk}^L = \lambda_{jk(0)}^L + \lambda_{jk(N)}^L; \lambda_{ik}^M = \lambda_{jk(0)}^M + \lambda_{jk(N)}^M; \tag{27}$$

$$\bar{\lambda}_{jk}^L = \bar{\lambda}_{jk(0)}^L + \bar{\lambda}_{jk(N)}^L; \bar{\lambda}_{ik}^M = \bar{\lambda}_{jk(0)}^M + \bar{\lambda}_{jk(N)}^M; \tag{28}$$

Index = 0? , as in (10) – (17), means the instantly elastic component, index = N ? (26), (28) – accumulated displacements:

$$\lambda_{jk(0)}^L = \frac{\Lambda_{jk(0)}^L}{P_k}; \quad (29)$$

$$\lambda_{jk(0)}^M = \frac{\Lambda_{jk(0)}^M}{P_k} . \quad (30)$$

$$\lambda_{jk(N)}^L = \frac{\Lambda_{jk(N)}^L}{P_k}; \quad (31)$$

$$\lambda_{jk(N)}^M = \frac{\Lambda_{jk(N)}^M}{P_k} . \quad (32)$$

$$\bar{\lambda}_{jk(0)}^L = \frac{\Lambda_{jk(0)}^L}{M_k}; \quad (33)$$

$$\bar{\lambda}_{jk(0)}^M = \frac{\Lambda_{jk(0)}^M}{M_k} \quad (34)$$

$$\bar{\lambda}_{jk(N)}^L = \frac{\Lambda_{jk(N)}^L}{M_k}; \quad (35)$$

$$\bar{\lambda}_{jk(N)}^M = \frac{\Lambda_{jk(N)}^M}{M_k} . \quad (36)$$

As in condition (20) using linear displacement of fracture points, displacements arising on N -th cycle replace the limit (under the action of a significant number of cycles) shows the displacement:

$$G_{max} = \text{ark cos} \left\{ 1 - \frac{1}{2S_{ML}^2} \sum_{j=1}^3 \left[\sum_{k=1}^3 P_k \left((\lambda_{jk(0)}^L + \lambda_{jk(gp)}^L - \lambda_{jk(0)}^M - \lambda_{jk(gp)}^M) + \right. \right. \right. \quad (37)$$

$$\left. \left. \left. + (\bar{\lambda}_{jk(0)}^L + \bar{\lambda}_{jk(gp)}^L - \bar{\lambda}_{jk(0)}^M - \bar{\lambda}_{jk(gp)}^M) e_k \right]^2 \right\} |_{max} \leq [G]$$

where indicated:

$$\lambda_{jk(gk)}^L = \frac{\Lambda_{jk(gp)}^L}{P_k}; \lambda_{jk(gp)}^M = \frac{\Lambda_{jk(gp)}^M}{P_k}; \bar{\lambda}_{jk(gp)}^L = \frac{\Lambda_{jk(gp)}^L}{M_k}; \bar{\lambda}_{jk(gp)}^M = \frac{\Lambda_{jk(gp)}^M}{M_k} \quad (38)$$

Using the coefficient of influence of cyclic creep (24), condition (37) can be written in this form:

$$G_{max} = \arccos \left\{ 1 - \frac{1}{2S_{ML}^2} \sum_{j=1}^3 \left[\sum_{k=1}^3 P_k \left(k_{jk}^L (\lambda_{jk(0)}^L + \bar{\lambda}_{jk(0)}^L e_k) - k_{jk}^M (\lambda_{jk(0)}^M + \bar{\lambda}_{jk(0)}^M e_k) \right) \right]^2 \right\} \leq [G] \quad (39)$$

A number of experimental studies have shown that the curve connecting the upper points of the cyclic creep diagram can be approximated with a sufficient degree of accuracy by the sum of exponential functions. As preliminary calculations indicated, the number of members of the sum is sufficient to be limited to three so that the approximation error does not exceed the instrumental error.

This is actually the use of the generalised Kelvin-Voigt model by formally replacing the force action time with the number of load cycles. Represent the displacement in formula (24) in this way:

$$\Lambda_{jk}^i(N) = \Lambda_{jk(0)}^i + \sum_{m=1}^n \Lambda_{jk(m)}^i \left[1 - \exp\left(-\frac{N}{N_m^i}\right) \right] \quad (40)$$

where $\Lambda_{jk(0)}^i$ – displacements that can be determined under static loads $\Lambda_{jk(m)}^i, N_m^i$ – coefficients that can be determined by cyclic creep curves; N – number of load cycles; m – exponent number; n – total number of exponents.

In this case, there should be a condition:

$$\sum_{m=1}^n \Lambda_{jk(m)}^i = \Lambda_{jk(gp)}^i \quad (41)$$

Dividing both sides (41) into P_k , the reduced movement of the cell was got: $\lambda_{jk(N)}^i$

$$\lambda_{jk}^i(N) = \lambda_{jk(0)}^i + \sum_{m=1}^n \lambda_{jk(m)}^i \left[1 - \exp\left(-\frac{N}{N_m^i}\right) \right] \tag{42}$$

Similarly, for reduced displacement $\bar{\lambda}_{jk}^i(N)$:

$$\bar{\lambda}_{jk}^i(N) = \bar{\lambda}_{jk(0)}^i + \sum_{m=1}^n \bar{\lambda}_{jk(m)}^i \left[1 - \exp\left(-\frac{N}{\bar{N}_m^i}\right) \right] \tag{43}$$

Substituting (43) into (10), the final form of the functional reliability condition using the criterion of maximum mutual displacements of fracture points under cyclic loads was obtained:

$$\Lambda_{max}(N) = \sqrt{\sum_{j=1}^3 \left[\sum_{k=1}^3 P_k \left(\left(\lambda_{jk(0)}^i + \sum_{m=1}^n \lambda_{jk(m)}^i \left[1 - \exp\left(-N / N_m^i\right) \right] \right) + \left(\bar{\lambda}_{jk(0)}^i + \sum_{m=1}^n \bar{\lambda}_{jk(m)}^i \left[1 - \exp\left(-N / \bar{N}_m^i\right) \right] \right) e_k \right) \right]^2} \Big|_{max} \leq [\Lambda] \tag{44}$$

Substituting (43) into (14), the final form of the criterion for the maximum angles of mutual rotation of the fracture parts under cyclic loads was obtained:

$$G_{max}(N) = \arccos \left\{ 1 - \frac{1}{2S_{ML}^2} \sum_{j=1}^3 \left[\sum_{k=1}^3 P_k \left(\left(\lambda_{jk(0)}^L + \sum_{m=1}^n \lambda_{jk(m)}^L \left[1 - \exp\left(-N / N_m^L\right) \right] - \left(-\lambda_{jk(0)}^M - \sum_{m=1}^n \lambda_{jk(m)}^M \left[1 - \exp\left(-N / N_m^M\right) \right] \right) + \left(\bar{\lambda}_{jk(0)}^L + \sum_{m=1}^n \bar{\lambda}_{jk(m)}^L \left[1 - \exp\left(-N / \bar{N}_m^L\right) \right] - \left(-\bar{\lambda}_{jk(0)}^M - \sum_{m=1}^n \bar{\lambda}_{jk(m)}^M \left[1 - \exp\left(-N / \bar{N}_m^M\right) \right] \right) \right) \right] \right\} \Big|_{max} \leq [G] \tag{45}$$

As an example, it can be considered the application of the above criteria to assess the permissible loads of the system “tibia with a fracture-fixation plate”. The following fracture points were considered: point M (medial, point near the fixation of the plates, except for plate 1L) and point L (lateral, point farthest from the plates). The external forces were applied in such a way that the directions of the projections of the displacement vectors of the point L, which arise due to individual forces and moments of forces, coincide (the most dangerous case). According to formula (3, 4), for an accurate assessment of the functional reliability of fracture fixation and determination of permissible loads, it is important to know 9 values of reduced

displacements λ_{jk}^i and 9 values of $\bar{\lambda}_{jk}^i$. Taking into account the displacements arising from the long-term impact of loads (18), the number of components of the given displacements increases to 36. Obviously, determining all the components, even using the digital method of recording displacements, is a rather complicated task. However, it turned out that the number of reduced displacements that affect the calculation results can be much smaller.

When lowering the number of reduced displacements that affect the calculation results, use the example of osteosynthesis systems in which bone plates are used to fix fractures. The given displacements were determined by the results of experiments for osseous medial plates with angular stability (hereinafter 2M), medial blocked plates (3M) and X-shaped medial blocked plates for open corrective osteotomy (4M). The considered plates showed the best results when tested at single loads.

The most dangerous fracture region is the one where under the action of loads the maximum mutual displacements of adjacent points occur. It is obvious (and this is confirmed experimentally) that in most cases the maximum displacements will occur at the point of fracture that is farthest from the fixation means (plate or rod apparatus of external fixation). Therefore, as the point "i" in the calculations of maximum displacements, it is necessary to take the point farthest from the latch. In the future, the movement would be denoted by points, unless it is necessary. The main contribution to the main displacement vector is made by the components $\Lambda_{X1}^i, \Lambda_{X2}^i, \Lambda_{Z1}^i, \Lambda_{Z2}^i, \Lambda_{Y3}^i$.

The first four components are longitudinal (along the X axis), and transverse (along the Z axis) displacement due to two forces P_1, P_2 . The fifth component is displacement in a plane perpendicular to the longitudinal axis of the bone, due to the moment of torsion M_3 . Table 1 shows the results of experiments conducted with the tibia with simulated fracture-fixation plate systems under load P_1, P_2, P_3 .

Table 1. Geometrical characteristics, displacements, and rotation angles of the tibia with fracture systems – fixation plate 2 under external loads.

| Plate | Impact force P_1 | | | | Fold force P_2 | | | Torsion force P_3 | | | |
|-------|--------------------|--------------------------------|------------------------|------------------------|------------------|--------------------------------|------------------------|---------------------|----------|--------------------------|-------------|
| | e_1 | Λ_{x1}^L / P_1 | Λ_{x1}^M / P_1 | Λ_{z1}^M / P_1 | e_2 | Λ_{x2}^L / P_2 | Λ_{z2}^L / P_2 | e_3 | S_{ML} | M_3 | $G_{YZ(3)}$ |
| | mm | $10^3 \text{ N}\cdot\text{mm}$ | | | mm | $10^3 \text{ N}\cdot\text{mm}$ | | mm | | $\text{N}\cdot\text{mm}$ | degree |
| 1L | 25.3 | 19.36 | 5.40 | 1.25 | 18.3 | 9.90 | 33.0 | 63.2 | 29.6 | 632 | 1.346 |
| 1M | 15.0 | 5.94 | 2.12 | 0.87 | 21.6 | 5.62 | 6.60 | 46.1 | 39.5 | 461 | 0.668 |
| 2M | 11.0 | 8.07 | 3.03 | 1.16 | 21.5 | 9.90 | 4.40 | 59.5 | 34.8 | 595 | 0.688 |
| 3M | 17.5 | 12.25 | 4.75 | 2.36 | 20.6 | 8.80 | 3.42 | 56.9 | 31.6 | 569 | 1.252 |
| 4M | 21.1 | 4.88 | 4.88 | 0.50 | 35.8 | 6.78 | 3.62 | 51.5 | 38.1 | 515 | 0.247 |

Table 2. Displacements of the fracture point L , most remote from the place of fixation by the plate.

| Plate | λ_{x1}^L | $\bar{\lambda}_{x1}^L$ | $\bar{\lambda}_{z1}^L$ | $\bar{\lambda}_{z2}^L$ | $\bar{\lambda}_{x2}^L$ | $\bar{\lambda}_{z2}^L$ | $\bar{\lambda}_{y3}^L$ |
|-------|--------------------------------|--|------------------------|--------------------------------|--|------------------------|------------------------|
| | $10^3 \text{ N}\cdot\text{mm}$ | $10^3 \text{ mm}/(\text{N}\cdot\text{mm})$ | | $10^3 \text{ N}\cdot\text{mm}$ | $10^3 \text{ mm}/(\text{N}\cdot\text{mm})$ | | |
| 1L | 5.40 | 0.552 | 0.049 | 32.1 | 0.541 | 0.049 | 1.100 |
| 1M | 2.12 | 0.255 | 0.058 | 5.35 | 0.260 | 0.058 | 0.999 |
| 2M | 3.03 | 0.458 | 0.105 | 2.13 | 0.460 | 0.105 | 0.702 |
| 3M | 4.75 | 0.429 | 0.134 | 0.64 | 0.427 | 0.134 | 1.213 |
| 4M | 0.80 | 0.193 | 0.023 | 2.77 | 0.189 | 0.023 | 0.319 |

An analysis of the results of the action of these forces separately and methods for calculating the reduced displacements from the results of measurements of the absolute displacements of various fracture points were presented. Reduced point movements M and L in the direction X under the force P_1 . Displacement Λ_{x1}^M is the result of longitudinal force P_1 , which causes the displacement of part of the fracture along the axis X , regardless of bending moment M_1 . It is equal to displacement Λ_{x1}^L of point L without taking into account the moment M_1 (parallel movement of the segment ML without taking into account rotation in the plane XZ). Therefore,

$$M_1 = P_1 e_1 \tag{46}$$

$$\lambda_{x1}^L = \lambda_{x1}^M = \frac{\Lambda_{x1}^M}{P_1} \tag{47}$$

Reduced displacement of point L in direction X under the influence of the moment M_1 . This displacement is equal $\Lambda_{x1}^L - \Lambda_{x1}^M$, and the corresponding reduced displacement:

$$\bar{\lambda}_{x1}^L = \frac{\Lambda_{x1}^L - \Lambda_{x1}^M}{P_1 e_1} \quad (48)$$

Reduced displacement of points L and M in direction Z under the influence of the moment M_1 . Because under the action of force P_1 lateral force in the direction Z is absent, cell displacement Λ_{z1}^L of point L in direction Z caused only by the influence of the moment M_1 . At small angles of rotation $\Lambda_{z1}^L = \Lambda_{z1}^M$, and the corresponding reduced displacement:

$$\bar{\lambda}_{z1}^L = \frac{\Lambda_{z1}^L}{P_1 e_1} = \frac{\Lambda_{z1}^M}{P_1 e_1} \quad (49)$$

Displacement of point L in direction Y under the influence of force P_1 . As the analysis of displacements of fracture points, displacements Λ_{y1}^L , Λ_{z1}^L due to force P_1 are dismissively small, which means that the quantities Λ_{y1}^L , Λ_{z1}^L are close to zero. No significant movement of fracture points in the direction Y gives reason to neglect the given displacement $\bar{\lambda}_{y1}^L$. Displacement of point L in direction Z under the influence of the force P_2 . Suppose that in the first state acts only force P_1 . In this state, the transverse force in the direction Z is absent and movement in this direction is caused only by a bending moment M_1 :

$$\Lambda_{z1}^L = \bar{\lambda}_{z1}^L M_1 = \bar{\lambda}_{z1}^L P_1 e_1 \quad (50)$$

Suppose that in the second state acts only the force P_2 . In this state, moving in the direction Z caused by the force P_2 and bending moment M_2 :

$$\Lambda_{z2}^L = \lambda_{z2}^L P_2 + \bar{\lambda}_{z2}^L M_2 = \lambda_{x2}^L P_2 + \bar{\lambda}_{x2}^L P_2 e_2 \quad (51)$$

Displacements from bending moments do not depend on the method of application of these moments, that is: $\bar{\lambda}_{z1}^L = \bar{\lambda}_{z2}^L$.

$$\bar{\lambda}_{z2}^L = \frac{\Lambda_{z1}^L}{P_1 e_1} \quad (52)$$

Substituting (52) into (53):

$$\lambda_{z2}^L = \frac{\Lambda_{z2}^L}{P_2} - \frac{\Lambda_{z1}^L e_2}{P_1 e_1} \quad (53)$$

Values of relations Λ_{z2}^L / P_2 and Λ_{z1}^L / P_1 are presented in Table. 1.

Displacement of point L in direction X under the force P_2 . The force P_2 causes no shift in direction X and $\Lambda_{x2}^M = 0$. Displacement Λ_{x2}^L only caused by the moment M_2 . In this case, the displacement is shown:

$$\bar{\lambda}_{x2}^L = \frac{\Lambda_{x2}^L}{P_2 e_2} \quad (54)$$

Notice, that $\bar{\lambda}_{x=1}^L \approx \bar{\lambda}_{x2}^L$ (Table 2). Deviations range from 0.44% (plate 2M) to 2.07% (plate 4M), which corresponds to the measurement error.

Displacement of point L in direction Y under the influence of force P_3 . It is defined that

$$tgG = \Lambda_{y3}^L / S_{ML}. \quad (55)$$

Thus, if:

$$\bar{\lambda}_{y3}^L = \frac{\Lambda_{y3}^L}{P_3 e_3} \quad (56)$$

then in the final form:

$$\bar{\lambda}_{y3}^L = tgG \frac{S_{ML}}{P_3 e_3} \quad (57)$$

The results of calculations using formulas (52)-(53), (53)-(57) using the data from Table 1 are given in Table 2. Displacement of point M in direction X under the force P_1 . Reduced displacement λ_{x1}^M , which corresponds with λ_{x1}^L , is given by the formula (47). Displacement of point M in direction Z under the effect of bending moments. Displacement of point M due to the bending moment, it does not depend on the method of application of this moment (that is, on the direction of the load that causes this moment), but the movement of points L and M in the transverse direction are equal. Therefore $\bar{\lambda}_{z1}^M = \bar{\lambda}_{z2}^M = \bar{\lambda}_{z1}^L = \bar{\lambda}_{z2}^L$.

Displacement of point M in direction Z under the force P_2 . Calculation of reduced displacements λ_{z2}^M is carried out in the same way as λ_{z2}^L :

$$\lambda_{z2}^M = \frac{\Lambda_{z2}^M}{P_2} - \frac{\Lambda_{z1}^M e_2}{P_1 e_1} \quad (58)$$

Relations $\Lambda_{z2}^M / P_2 = \Lambda_{z2}^L / P_2$ and λ_{z1}^M / P_1 are given in the Table 1. Displacement of point M under the influence of force P_3 . The center of rotation of the fracture under the action of force P_3 coincides with the place of fixation of the fracture by the plate, therefore absolute and reduced moving points M due to the action of this force, it is extremely small, which is confirmed by torsion experiments. Reduced displacement of point M , calculated by formulas (47), (53), placed in the Table 3.

Table 3. The reduced displacements of the fracture point M close to the place of fixation by the plate.

| Plate | λ_{x1}^M | $\bar{\lambda}_{z1}^M$ | λ_{z2}^M | $\bar{\lambda}_{z2}^M$ |
|-------|---------------------------------------|---|---------------------------------------|---|
| | $\times 10^3, \text{N}\cdot\text{mm}$ | $\times 10^3, \text{mm} / (\text{N}\cdot\text{mm})$ | $\times 10^3, \text{N}\cdot\text{mm}$ | $\times 10^3, \text{mm} / (\text{N}\cdot\text{mm})$ |
| 1L | 5.40 | 0.049 | 32.1 | 0.049 |
| 1M | 2.12 | 0.058 | 5.35 | 0.058 |
| 2M | 3.03 | 0.105 | 2.13 | 0.105 |
| 3M | 4.75 | 0.134 | 0.64 | 0.134 |
| 4M | 0.80 | 0.023 | 2.77 | 0.023 |

The matrix representation of the reduced displacements of the points L and M . The reduced displacements are conveniently represented in the form of matrices (59) – (62). The negligibly small quantities in these matrices are indicated by zeros.

$$\begin{pmatrix} \lambda_{x1}^L & 0 & 0 \\ 0 & 0 & \lambda_{z2}^L \\ 0 & 0 & 0 \end{pmatrix}; \quad (59)$$

$$\begin{pmatrix} \bar{\lambda}_{x1}^L & 0 & \bar{\lambda}_{z1}^L \\ \bar{\lambda}_{x2}^L & 0 & \bar{\lambda}_{z2}^L \\ 0 & \bar{\lambda}_{y3}^L & 0 \end{pmatrix}; \quad (60)$$

$$\begin{pmatrix} \lambda_{x1}^M & 0 & 0 \\ 0 & 0 & \lambda_{z2}^M \\ 0 & 0 & 0 \end{pmatrix} \quad (61)$$

$$\begin{pmatrix} 0 & 0 & \bar{\lambda}_{z1}^M \\ 0 & 0 & \bar{\lambda}_{z2}^M \\ 0 & 0 & 0 \end{pmatrix} \quad (62)$$

The rigidity conditions of the systems “fracture – plate” at one-time loads. Given only those given displacements $\lambda_{jk}^i, \bar{\lambda}_{jk}^i$, which are different from zero in matrices (59) – (62), the conditions of functional reliability (3, 4), (12) at single loads are significantly simplified:

$$\Lambda_{max} = \sqrt{\left[P_1(\lambda_{x1}^L + \bar{\lambda}_{x1}^L e_1) + P_2 \bar{\lambda}_{x2}^L e_2 \right]^2 + \left[P_2(\bar{\lambda}_{y3}^L e_3) \right]^2 + \left[P_1(\bar{\lambda}_{z1}^L e_1) + P_2(\lambda_{z2}^L + \bar{\lambda}_{z2}^L e_2) \right]^2} \leq [\Lambda] \quad (63)$$

$$G_{max} = \arccos \left\{ 1 - \frac{1}{2S_{ML}^2} \left[(P_1 \bar{\lambda}_{x1}^L e_1 + P_2 \bar{\lambda}_{x2}^L e_2)^2 + (P_3 \bar{\lambda}_{y3}^L e_3)^2 \right] \right\} \Big|_{max} \leq (G) \quad (64)$$

The stiffness conditions for the systems “fracture – plate” under cyclic loads (23), (37) are reduced to the form (16), (37) without taking into account small reduced displacements in matrices (59) – (62). Note that the displacements of these points in the corresponding directions due to creep are also close to zero (they are at the level of instrumental error). To take into account the influence of cyclic loads, let's assume that the ratio between the projections $\Lambda_{jk(gp)}^L$

and $\Lambda_{jk(0)}^L$ in coefficient (24), depend little on the direction of the coordinate axis and depend only on the direction of the reduced force. In this case, complete displacements arising due to force P_k , can be calculated by introducing the same coefficients in (24):

$$k_{xk}^L = k_{yk}^L = k_{zk}^L = k_k^L = 1 + \frac{\Lambda_{k(gp)}^i}{\Lambda_{k(0)}^i} \quad (65)$$

The error that may arise due to this assumption will not be significant, since the values of the coefficients k_k^i are in rather narrow ranges: 1.28 ... 1.31 for a 2M plate; 1.21 ... 1.625 for the 3M plate and 1.29 ... 1.32 for the 4M plate (Table 4) It should be noted that a large value k_k^i for a 4M plate does not indicate a high level of creep of this system; in this system, the cyclic creep strains are the smallest. Given these assumptions, the rigidity condition (23), a generalisation of condition (63) for the case of cyclic creep for a system with plates, will have the form:

$$\Lambda_{max} = \sqrt{\left[P_1 k_1^L (\lambda_{x1}^L + \bar{\lambda}_{x1}^L e_1) + P_2 k_2^L \bar{\lambda}_{x2}^L e_2 \right]^2 + \left[P_3 k_3^L \bar{\lambda}_{y3}^L e_3 \right]^2 + \left[P_1 k_1^L \bar{\lambda}_{z1}^L e_1 + P_2 k_2^L (\lambda_{z2}^L + \bar{\lambda}_{z2}^L e_2) \right]^2} \Big|_{max} \leq [\Lambda] \quad (66)$$

Similarly, given that $\lambda_{x1}^L = \lambda_{x1}^M; \bar{\lambda}_{z1}^L = \bar{\lambda}_{z2}^M; \lambda_{z2}^L = \lambda_{z2}^M; \bar{\lambda}_{z2}^L = \bar{\lambda}_{x2}^M$, condition (37) and generalised condition (64) for the case of cyclic creep for a system with plates will have the form:

$$G_{max} = \arccos \left\{ 1 - \frac{1}{2S_{ML}^2} \left[(P_1 k_1^L \bar{\lambda}_{x1}^L e_1 + P_2 k_2^L \bar{\lambda}_{x2}^L e_2)^2 + (P_3 k_3^L \bar{\lambda}_{y3}^L e_3)^2 \right] \right\} \leq [G] \quad (67)$$

Table 4. Coefficient values $k_{jk}^i, N_m^j, \bar{N}_{m^m}^j$ of functional reliability conditions (66) and (67).

| Characteristic | Plates | | |
|-------------------------------|--------|------|------|
| | 2M | 3M | 4M |
| Stress k_{j1}^i | 1.29 | 1.21 | 1.31 |
| Bending k_{j2}^i | 1.28 | 1.25 | 1.29 |
| Torsion k_{j3}^i | 1.31 | 1.21 | 1.32 |
| Coefficients N_1, \bar{N}_1 | 7 | 7 | 12 |
| Coefficients N_2, \bar{N}_2 | 28 | 28 | 28 |
| Coefficients N_3, \bar{N}_3 | 70 | 70 | 70 |

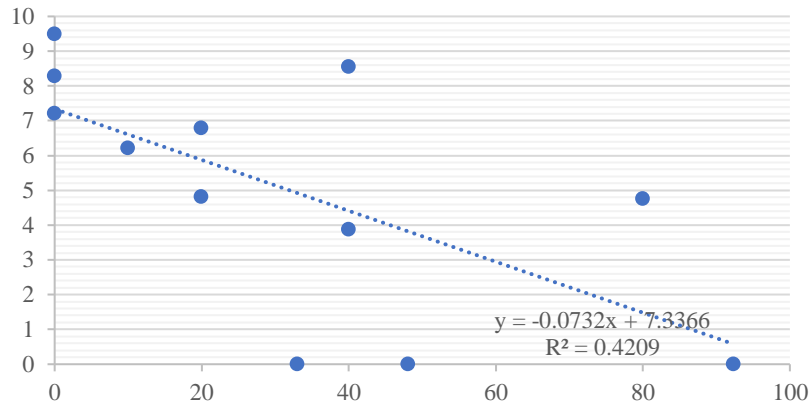
Using the criterion of maximum linear displacement recorded in the form (3), and the value of reduced displacements given in Tables 2 and 3, were calculated the permissible loads $P_{1(dop)}, P_{2(dop)}, P_{3(dop)}$ with their simultaneous action. The calculation results are given in Table 5. For the permissible mutual movement of the fracture points was taken $[\Delta] = 1mm$. Using the criterion for the maximum mutual angle of rotation of the fracture parts recorded in the formula (8), and the values of the reduced displacements given in Table 2 and 3, permissible loads calculated $P_{1(dop)}, P_{2(dop)}, P_{3(dop)}$ with their simultaneous action. Permissible loads calculated according to the specified condition when $[G] = 3^\circ$ had significantly larger values than those shown in Table 5. Because the permissible loads were chosen, calculated according to the permissible linear displacements under the condition (3, 4).

Table 5. Permissible loads $P_{1(dop)}$, $P_{2(dop)}$, $P_{3(dop)}$, not leading to mutual displacement of fracture points greater than 1 mm when the fracture is fixed by various types of plates.

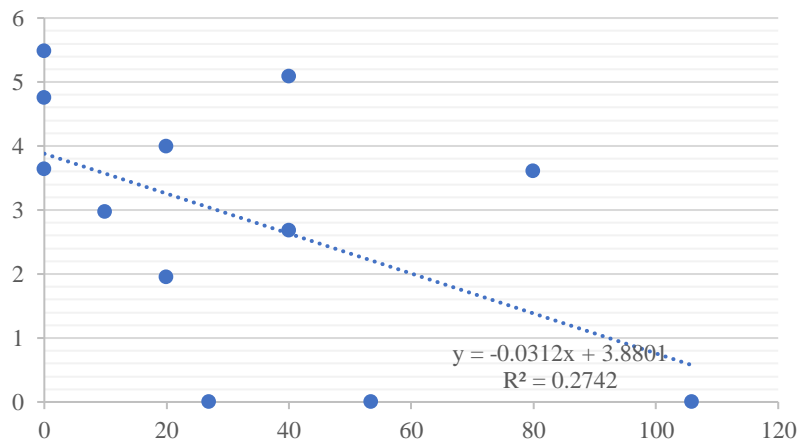
| Plate 2M | | | Plate 3M | | | Plate 4M | | |
|--------------|--------------|--------------|--------------|--------------|--------------|--------------|--------------|--------------|
| $P_{1(dop)}$ | $P_{2(dop)}$ | $P_{3(dop)}$ | $P_{1(dop)}$ | $P_{2(dop)}$ | $P_{3(dop)}$ | $P_{1(dop)}$ | $P_{2(dop)}$ | $P_{3(dop)}$ |
| 0 | 0 | 9.50 | 0 | 0 | 5.49 | 0 | 0 | 20.89 |
| | 40.0 | 8.56 | | 40.0 | 5.09 | | 40.0 | 190.90 |
| | 80.0 | 4.75 | | 80.0 | 3.61 | | 100.0 | 13.44 |
| | 92.4 | 0 | | 105.9 | 0 | | 130.0 | 0 |
| 60 | 0 | 8.28 | 40 | 0 | 4.76 | 60 | 0 | 19.98 |
| | 20.0 | 6.79 | | 20.0 | 4.00 | | 30.0 | 17.94 |
| | 40.0 | 3.88 | | 40.0 | 2.68 | | 60.0 | 14.07 |
| | 48.1 | 0 | | 53.5 | 0 | | 94.2 | 0 |
| 80 | 0 | 7.20 | 60 | 0 | 3.64 | 100 | 0 | 18.23 |
| | 10.0 | 6.21 | | 10.0 | 2.97 | | 20.0 | 16.16 |
| | 20.0 | 4.81 | | 20.0 | 1.95 | | 40.0 | 13.03 |
| | 33.0 | 0 | | 27.0 | 0 | | 69.1 | 0 |
| 122.6 | 0 | 0 | 80.1 | 0 | 0 | 203.7 | 0 | 0 |

For clarity, the data given in Table 5 is presented in the form of three-dimensional diagrams (limiting areas) that limit the areas of permissible loads (Fig. 5). Any point located under each of the surfaces corresponds to three values of the loads P_1 , P_2 and P_3 , the combined action of which does not lead to the occurrence of displacements and rotation angles of the fracture parts that are larger than permissible: $\Lambda < 1mm$ and $[G] < 3^\circ$. If the point belongs to the surface, then this combination P_1, P_2, P_3 causes the cell displacement $\Lambda = 1mm$. In the case when the point is outside the boundary surface, such combination of loads is dangerous, while moving the cell fracture point distant from the plate $\Lambda > 1mm$.

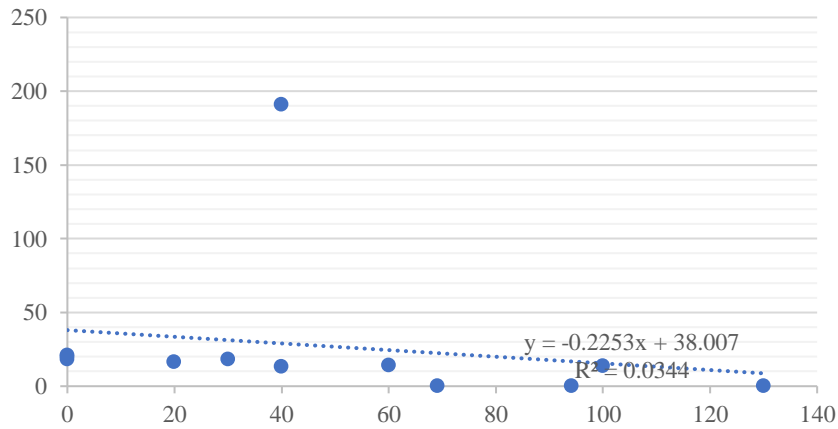
Figure 5. Area of permissible loads $P_{1(dop)}, P_{2(dop)}, P_{3(dop)}$, not leading to physiologically dangerous displacements larger than $\Lambda = 1mm$.



2M



3M



4M

CONCLUSION

The value of permissible loads calculated using the given deformations only corresponds to the initial state of bone regeneration. The process of rehabilitation of the injured is accompanied by exposure of limbs to cyclically acting loads (walking, exercise). To determine the permissible loads for the later stages of fracture fusion, it is necessary to take into account the kinetics of changes in the deformation properties of bone tissue in the fracture region during its regeneration. Calculation of permissible loads provided that the force P_3 acts at a distance $e_3 = 150mm$ from the longitudinal axis of the system (lateral load on the distal region of the 1st metatarsal bone). It should be noted that the given deformations (Tables 2 and 3) were determined experimentally on full-scale bone specimens with simulated fractures with diastases (distances between the edges of the fracture) not filled with bone regenerate.

This fractured state corresponds only to the initial stages of fusion when the regeneration is absent or its mechanical properties do not affect the deformation (displacement) of the fracture point under the influence of physiological loads. The prospects were determined by the need to form adaptive potential, which will allow athletes to maintain positive dynamics of performances in the future at the level of international competitions.

Declaration of Competing Interest

The authors declared no potential conflicts of interest with respect to the research, authorship, and/or publication of this article.

Funding

This research did not receive any specific grant from funding agencies in the public, commercial, or not-for-profit sectors

REFERENCES

- Abassi, M., Bleakley, C., & Whiteley, R. (2019). Athletes at late stage rehabilitation have persisting deficits in plantar- and dorsiflexion, and inversion (but not eversion) after ankle sprain. *Physical Therapy in Sport*, 38, 30–35. <https://doi.org/10.1016/j.ptsp.2019.04.015>
- Allado, E., Poussel, M., Hily, O., & Chenuel, B. (2022). The interest of rehabilitation of respiratory disorders in athletes: Myth or reality? *Annals of Physical and Rehabilitation Medicine*, 65(4) <https://doi:10.1016/j.rehab.2020.101461>

- Arvinen-Barrow, M., Clement, D., Hamson-Utley, J. J., Zakrajsek, R. A., Lee, S.-M., Kamphoff, C., Martin, S. B. (2015). Athletes' use of mental skills during sport injury rehabilitation. *Journal of Sport Rehabilitation*, 24(2), 189–197. <https://doi.org/10.1123/jsr.2013-0148>
- Arvinen-Barrow, M., Massey, W. V., & Hemmings, B. (2014). Role of sport medicine professionals in addressing psychosocial aspects of sport-injury rehabilitation: Professional athletes' views. *Journal of Athletic Training*, 49(6), 764–772. <https://doi.org/10.4085/1062-6050-49.3.44>
- Bakrac, N.D. (2003). Dynamics of muscle strength improvement during isokinetic rehabilitation of athletes with ACL rupture and chondromalacia patellae. *Journal of Sports Medicine and Physical Fitness*, 43(1), 69–74.
- Bejar, M. P., Raabe, J., Zakrajsek, R. A., Fisher, L. A., & Clement, D. (2019). Athletic trainers' influence on National collegiate athletic Association division I athletes' basic psychological needs during sport injury rehabilitation. *Journal of Athletic Training*, 54(3), 245–254. <https://doi.org/10.4085/1062-6050-112-18>
- Bjerke, W., Steinman, S., & Cotto, V. (2014). Cardiac rehabilitation programmes for low-risk patients and leisure athletes: A potential paradox. *International Journal of Therapy and Rehabilitation*, 21(2), 84–90. <https://doi.org/10.12968/ijtr.2014.21.2.84>
- Carlson, C. (2009). Axial back pain in the athlete: Pathophysiology and approach to rehabilitation. *Current Reviews in Musculoskeletal Medicine*, 2(2), 88–93. <https://doi.org/10.1007/s12178-009-9050-y>
- Gart, M. S., & Wiedrich, T. A. (2017). Therapy and Rehabilitation for Upper Extremity Injuries in Athletes. *Hand Clinics*, 33(1), 207–220. <https://doi.org/10.1016/j.hcl.2016.08.016>
- Grindem, H., Arundale, A. J. H., & Ardern, C. L. (2018). Alarming underutilisation of rehabilitation in athletes with anterior cruciate ligament reconstruction: Four ways to change the game. *British Journal of Sports Medicine*, 52(18), 1162–1163. <https://doi.org/10.1136/bjsports-2017-098746>
- Hagerman, G. R., Atkins, J. W., & Dillman, C. J. (1995). Rehabilitation of chondral injuries and chronic degenerative arthritis of the knee in the athlete. *Operative Techniques in Sports Medicine*, 3(2), 127–135. [https://doi.org/10.1016/S1060-1872\(95\)80039-5](https://doi.org/10.1016/S1060-1872(95)80039-5)
- Hart, A. L., Malone, T. R., & English, T. (1998). Shoulder function and rehabilitation implications for the wheelchair racing athlete. *Topics in Spinal Cord Injury Rehabilitation*, 3(3), 50–65.
- Hawson, S. T. (2011). Physical Therapy and Rehabilitation of the Foot and Ankle in the Athlete. *Clinics in Podiatric Medicine and Surgery*, 28(1), 189–201. <https://doi.org/10.1016/j.cpm.2010.09.005>
- Hilliard, R. C., Blom, L., Hankemeier, D., & Bolin, J. (2017). Exploring the relationship between athletic identity and beliefs about rehabilitation overadherence in college athletes. *Journal of Sport Rehabilitation*, 26(3), 208–220. <https://doi.org/10.1123/jsr.2015-0134>
- Karpiel, I., Ziebinski, A., Kluszczynski, M., & Feige, D. (2021). A Survey of Methods and Technologies Used for Diagnosis of Scoliosis. *Sensors*, 21(24), 8410. <https://doi.org/10.3390/s21248410>
- Lu, F. J. H., & Hsu, Y. (2013). Injured athletes' rehabilitation beliefs and subjective well-being: The contribution of hope and social support. *Journal of Athletic Training*, 48(1), 92–98. <https://doi.org/10.4085/1062-6050-48.1.03>
- Malempati, C., Jurjans, J., Noehren, B., Ireland, M. L., & Johnson, D. L. (2015). Current rehabilitation concepts for anterior cruciate ligament surgery in athletes. *Orthopedics*, 38(11), 689–696. <https://doi.org/10.3928/01477447-20151016-07>
- Qiao, Y., Zhang, L., & Zhang, B. (2022). Rehabilitation treatment of muscle strain in athlete training under intelligent intervention. *Computational and Mathematical Methods in Medicine*, 2022. <https://doi.org/10.1155/2022/5403681>
- Riley, A. H., & Callahan, C. (2019). Shoulder rehabilitation protocol and equipment fit recommendations for the wheelchair sport athlete with shoulder pain. *Sports Medicine and Arthroscopy Review*, 27(2), 67–72. <https://doi.org/10.1097/JSA.0000000000000232>

- Rossi, M. J., & Brand, J. C. (2022). Rehabilitation is the critical ingredient to optimize return to sport in athletes. *Arthroscopy – Journal of Arthroscopic and Related Surgery*, 38(1), 7-9. <https://doi:10.1016/j.arthro.2021.11.016>
- Rudenko, R., Mahliovanyy, A., Shyyan, O., & Prystupa, T. (2015). Physical rehabilitation and thermoregulatory processes in athletes with disabilities. *Journal of Physical Education and Sport*, 15(4), 730–735. <https://doi.org/10.7752/jpes.2015.04111>.
- Wasik, J., Motow-Czyz, M., Shan, G.B., & Kluszczynski, M. (2015). Comparative analysis of body posture in child and adolescent taekwon-do practitioners and non-practitioners. *Ido Movement for Culture-Journal of Martial Arts Anthropology*, 15(3), 35-40. <https://doi.org/10.14589/ido.15.3.5>
- Wilk, K. E., Arrigo, C. A., Hooks, T. R., & Andrews, J. R. (2016). Rehabilitation of the Overhead Throwing Athlete: There Is More to It Than Just External Rotation/Internal Rotation Strengthening. , 8(3), S78–S90. <https://doi.org/10.1016/j.pmrj.2015.12.005>.